Evidence for the binding mode of porphyrins to G-quadruplex DNA†

Chunying Wei,*[a] Guoqing Jia,[b] Jun Zhou,[b] Gaoyi Han[a] and Can Li*[b]

Received 16th January 2009, Accepted 20th February 2009
First published as an Advance Article on the web 13th March 2009
DOI: 10.1039/b901027k

Interactions of porphyrin derivatives 5,10,15,20-tetrakis(*N*-methylpyridinium-4-yl)-21*H*,23*H*-porphyrin (TMPyP4) and 5,10,15,20-tetrakis(*N*-propylpyridinium-4-yl)-21*H*,23*H*-porphyrin (TPrPyP4) with human telomeric $AG_3(T_2AG_3)_3$ G-quadruplex DNAs in 150 mM K^+-containing buffer in the presence or absence of 40% molecular crowding agent poly(ethylene glycol) (PEG 200) were studied by absorption titration fitting and time-resolved fluorescence spectroscopy. The results show that two TMPyP4 (or TPrPyP4) molecules bind to antiparallel/parallel hybrid structure of $AG_3(T_2AG_3)_3$ G-quadruplex by end-stacking and outside groove binding modes in the absence of PEG. Interestingly, in the presence of PEG one porphyrin molecule is stacked between two parallel $AG_3(T_2AG_3)_3$ G- quadruplexes to form a sandwich structure, another porphyrin molecule is bound to the groove of the G-quadruplex. The interactions of TMPyP4 with different structures of $AG_3(T_2AG_3)_3$ G-quadruplex are non cooperative, the binding constants of two independent binding sites are 1.07×10^6 and 4.42×10^8 M^{-1} for an antiparallel/parallel hybrid structure of $AG_3(T_2AG_3)_3$, 8.67×10^5 and 2.26×10^8 M^{-1} for parallel-stranded $AG_3(T_2AG_3)_3$ G-quadruplex. Conversely, the two binding sites are cooperative for TPrPyP4, the apparent association constants are 5.58×10^6 and 1.24×10^7 M^{-1} for parallel-stranded and antiparallel/parallel hybrid structures of $AG_3(T_2AG_3)_3$ G-quadruplex, respectively.

1. Introduction

Human chromosome ends are protected with kilobases repeats of TTAGGG. Telomere DNA shortens at replication.[1] This shortening in most tumor cells is compensated by telomerase that adds telomere repeats to the 3′ end of the G-rich telomere strand.[2] Four TTAGGG repeats can fold into G-quadruplex that is a poor substrate for telomerase.[3] This property has been suggested to regulate telomerase activity *in vivo* and telomerase inhibition *via* G-quadruplex stabilization is considered a therapeutic strategy against cancer.[4–8] Intense interest has arisen recently in searching for small molecules that stabilize G-quadruplex to inhibit telomere elongation by telomerase. The porphyrin derivative 5,10,15,20-tetrakis-(*N*-methylpyridinium-4-yl)-21*H*,23*H*-porphyrin (TMPyP4) has been extensively studied as a quadruplex-binding ligand since it can inhibit the activity of telomerase upon binding to human telomeric G-quadruplex DNAs.[9,10]

G-quadruplex DNAs contain multiple G-quartets, which are planar arrangements of four Hoogsteen hydrogen-bonded guanines (Scheme 1A). The size of a porphyrin ring is similar to that of a G-quartet, hence the stability of G-quadruplex DNA by porphyrin is due mainly to a π–π stacking interaction between the porphyrin ring and the G-quartet. Two main models have been proposed for binding TMPyP4 to different types of G-quadruplexes *in vitro*, namely, intercalative binding between adjacent G-quartets[11–13] and end-stacking on the G-quartets.[13–16] However, some other binding modes except π–π stacking interaction between the porphyrin ring and G-quartet have also been suggested. For example, Neidle, *et al.* recently reported an X-ray structure of a G-quadruplex-TMPyP4 complex,[17] indicating that two TMPyP4 molecules fail to interact directly with G-quartets in the G-quadruplex.

The aqueous environment in living cells is highly crowded. The total concentration of proteins, nucleic acids, and polysaccharides can reach 300–400 g L^{-1} whereas in most *in vitro* biochemical studies it was less than 1 g L^{-1}.[18–20] In general, crowding may significantly alter the rates, equilibria, and mechanisms of biomolecular reactions.[20–22] The effect of crowding on the G-quadruplex have been reported. It was observed that molecular crowding induces structural transition from the antiparallel to the parallel G-quadruplex in human $AG_3(T_2AG_3)_3$ telomeric DNA.[23–25]

However, until now studies on the interaction of TMPyP4 with G-quadruplex have been conducted only in dilute buffer solution. In order to understand the effect of the crowding agent on the interaction between porphyrin and G-quadruplex DNA, here we study the interaction of TMPyP4 (Scheme 1B) with $AG_3(T_2AG_3)_3$ G-quadruplex in 150 mM KCl buffer in the presence of 40% molecular crowding agent poly(ethylene glycol) (PEG 200).

In addition, it would also be of some interest to compare the interactions of porphyrin derivatives with the different

[a] *Key Laboratory of Chemical Biology and Molecular Engineering of Ministry of Education, Institute of Molecular Science, Shanxi University, Taiyuan, 030006, China. E-mail: weichuny@sxu.edu.cn; Fax: (+) 86-351-7011022; Tel: (+)86-351-7010699*
[b] *State Key Laboratory of Catalysis, Dalian Institute of Chemical Physics, Chinese Academy of Sciences, Dalian, 116023, China. E-mail: canli@dicp.ac.cn; Fax: (+) 86-411-84694447; Tel: (86)-411-84379070*

† Electronic supplementary information (ESI) available: EPS's of absorption spectra of TMPyP4 and TPrPyP4 (Fig. S1), Scatchard plots (Fig. S2); Plots of *r* (moles of bound TMPyP4/1 mol of G-quadruplexes) *versus* [TMPyP4]free (Fig. S3).. See DOI: 10.1039/b901027k

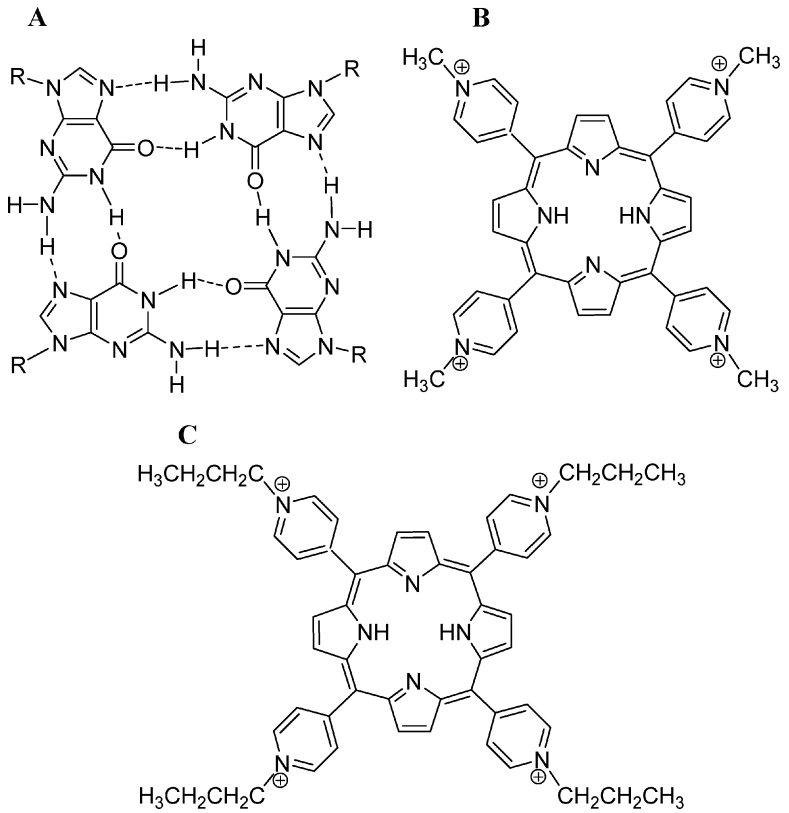

Scheme 1 Structures of G-quartets(A), TMPyP4(B) and TPrPyP4(C).

cation side arm in porphyrin core with the G-quadruplex. To clarify the effect of the cation side arm in the porphyrin core, the interaction of another porphyrin derivative, 5,10,15,20-tetrakis(*N*-propylpyridinium-4-yl)-21*H*,23*H*-porphyrin (TPrPyP4) bearing *N*-propylpyridinium cationic side arms (Scheme 1C), with $AG_3(T_2AG_3)_3$ G-quadruplex was also studied here in the same solution conditions as those of TMPyP4-$AG_3(T_2AG_3)_3$. On the basis of circular dichroism (CD), visible absorption and steady-state and time-resolved fluorescence spectroscopies, the binding stoichiometries, binding constants and binding modes of TMPyP4 and TPrPyP4 with $AG_3(T_2AG_3)_3$ G-quadruplex were first studied in detail, and their binding behaviour was compared in the buffer with or without 40% PEG.

2 Experimental

2.1 Materials

The DNA oligonucleotide $AG_3(T_2AG_3)_3$ was purchased from the SBS Genetech Co., Ltd. (China) in a PAGE-purified form. Single-strand concentrations were determined by measuring the absorbance at 260 nm at a high temperature using single-strand extinction coefficients at 260 nm 228 500 M^{-1} cm^{-1}.[13] The formation of G-quadruplexes was carried out as follows: the oligonucleotide samples, dissolved in a buffer solution consisting of 10 mM Tris-HCl, 1 mM EDTA and 150 mM KCl at pH 7.5, were heated to 90 °C for 5 min, gently cooled to room temperature, and then incubated at 4 °C overnight.

TMPyP4 was purchased in the form of tetra-*p*-tosylate salt from Tokyo Kasei Kogyo Co., Ltd. (Japan). TPrPyP4 was synthesized according to the literature procedure.[26] The concentrations of TMPyP4 and TPrPyP4 were determined by measuring the absorbance at 424 and 423 nm with an extinction coefficient of 2.26×10^5 and 2.1×10^5 M^{-1} cm^{-1}, respectively.[13,27]

Circular dichroism

CD experiments were performed at room temperature using a Jasco-820 spectropolarimeter. For each sample, at least three spectrum scans were accumulated in a 1 cm-path length cell at a scanning rate of 50 nm min^{-1} and the data were obtained with a 1 nm bandwidth. The concentrations of G-quadruplexes are 10 μM. The scan of the buffer alone was subtracted from the average scan for each sample.

Absorption spectroscopy

Absorption spectra were measured on a HP 8453 ChemStation with 1 cm path-length quarter cell. Visible absorption titrations were terminated when the wavelength and intensity of the absorption band for porphyrin did not change any more upon three successive additions of G-quadruplex.

The titration data obtained were applied to construct Scatchard eqn (1) and (2) where r is the number of moles of porphyrin bound to 1 mol of G-quadruplex (C_b/C_{DNA}), n is the number of equivalent binding sites, and K is the ligand affinity for those sites.[11,28] The concentrations of free porphyrin (C_f) and bound porphyrin (C_b) are calculated using

$C_f = C(1 - \alpha)$ and $C_b = C - C_f$, respectively, where C is the total porphyrin concentration (3.5 μM). The fraction of bound porphyrin (α) was calculated using the equation, $\alpha = (A_f - A)/(A_f - A_b)$,[21] where A_f and A_b are the absorbance of the free and fully bound porphyrin at the Soret maximum of porphyrin, respectively, and A is the absorbance at the Soret maximum of porphyrin at any given point during the titration.

$$\frac{r}{C_f} = nK - Kr \quad (1)$$

$$r = \frac{n_1 K_1 C_f}{1 + K_1 C_f} + \frac{n_2 K_2 C_f}{1 + K_2 C_f} \quad (2)$$

eqn (1) is the Scatchard plot, and the plot of r/C_f *versus* r gives a linear curve when there is only one type of binding, deviations from linearity can arise from the unequal association constants. Thus, K is obtained from the Scatchard analysis as an apparent binding constant. If there are two types of binding sites, and each binding site does not influence the bindings on the other sites (non cooperative binding), Scatchard analysis can be expressed in eqn (2) that is the direct plot, from which the number of each binding site (n) and their binding constant (K) can be obtained by nonlinear regression. Linear and nonlinear regression analyses of the data were performed in the Origin 7.0 software.

The percent hypochromicity of the Soret band of porphyrin can be calculated using hypochromicity % = $[(\varepsilon_f - \varepsilon_b)/\varepsilon_f] \times 100$, where $\varepsilon_b = A_b/C_b$.[13]

Two series of solutions were used for the continuous variation analysis experiments: one with a varying mole fraction of porphyrin and G-quadruplex and another with varying concentrations of porphyrin, while the sum of the porphyrin and G-quadruplex concentration was kept at 10 μM. Absorption difference spectra were obtained by subtraction of the absorption spectrum for porphyrin in the absence of G-quadruplexes from that in the presence of G-quadruplexes. The cells were cleaned with concentrated HCl between measurements to remove all traces of porphyrin that easily deposits on the quartz cell.

The difference in the maximum absorbance values at two wavelengths was plotted *versus* the porphyrin mole fraction to generate a Job plot,[13,29,30] which corresponds to the absorbance difference values between 445 and 423 nm, 444 and 420 nm for TMPyP4, between 445 and 422 nm, 445 and 421 for TPrPyP4 in the presence and absence of 40% PEG, respectively.

Steady and time-resolved fluorescence spectroscopy

Steady and time-resolved fluorescence measurements were performed using FL920 fluorescence lifetime spectrometer (Edinburgh Instruments, Livingston, UK) operating in the time-correlated single photon counting (TCSPC) mode. The excitation wavelength is set at 430 nm, and the slit width is 2 nm for both excitation and emission for steady fluorescence experiment. The samples were excited by 406.8 nm picosecond pulsed diode laser with a pulse width of 64.2 ps and the emission was observed at multiple wavelengths for a time-resolved fluorescence measurement. All decay traces were measured using 4096-channel analyzer. The time resolution per channel was 24 ps. The number of peak counts was approximately 7000. For data analyses, commercial software by Edinburgh Instruments was used. The data were fitted using a reconvolution method of the instrument response function (IRF) producing χ^2 fitting values of 1–1.3.

3. Results and discussion

3.1 Structural characterization of G-quadruplex DNAs

CD has been used to examine the structures of quadruplex DNAs.[31] Fig. 1 shows CD spectra of $AG_3(T_2AG_3)_3$ in K^+ buffer with or without 40% PEG. In the absence of PEG the CD spectrum of $AG_3(T_2AG_3)_3$ presents a strong positive peak at 291 nm associated with a weak shoulder peak at 250 nm and a weak negative band at 236 nm, which is the hybrid of a parallel/antiparallel-stranded G-quadruplex.[32] However a positive band at 268 nm and a negative band at 241 nm are observed in the presence of PEG, indicating that PEG induces $AG_3(T_2AG_3)_3$ to form the parallel-stranded G-quadruplex, which is consistent with a previously reported result.[24] The folded structures of $AG_3(T_2AG_3)_3$ in the presence and absence of PEG are shown in Scheme 2.

3.2. Binding stoichiometries and binding constants of porphyrins to G-quadruplexes

As described above, $AG_3(T_2AG_3)_3$ forms the parallel/antiparallel-stranded hybrid and parallel-stranded G-quadruplexes in the K^+-containing solution in the absence and presence of 40% PEG, respectively. To investigate the binding behavior of both TMPyP4 and TPrPyP4 to the different structure of $AG_3(T_2AG_3)_3$ G-quadruplex, firstly we measured the visible absorption titration spectra of porphyrins by addition of the different concentrations of the G-quadruplex (Fig. 2).

The results show 15 nm red shift and 65% hypochromicity in the absence of PEG, and 13 nm red shift and 50% hypochromicity in the presence of PEG in the Soret band of TMPyP4 at the end of titration (Fig. 2A, B), whereas a 14 nm red shift and 62% hypochromicity and 10 nm red shift and 45% hypochromicity were observed in the absence and presence of PEG in the Soret band of TPrPyP4 at the end of titration, respectively (Fig. 2C, D). In addition, compared with

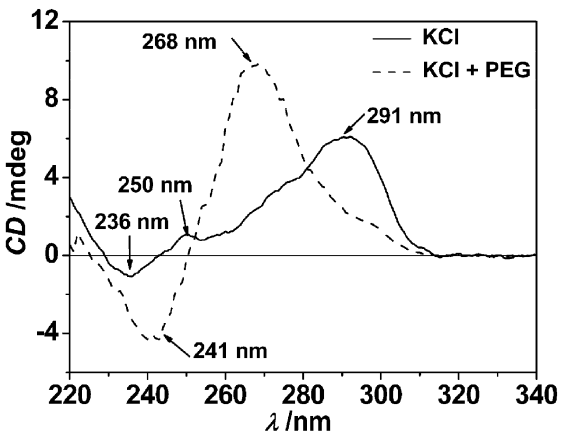

Fig. 1 CD spectra of $AG_3(T_2AG_3)_3$ G-quadruplexes at a concentration of 10 μM in 10 mM Tris-HCl (pH 7.5), 150 mM KCl and 1 mM EDTA buffer in the presence or absence of 40% PEG.

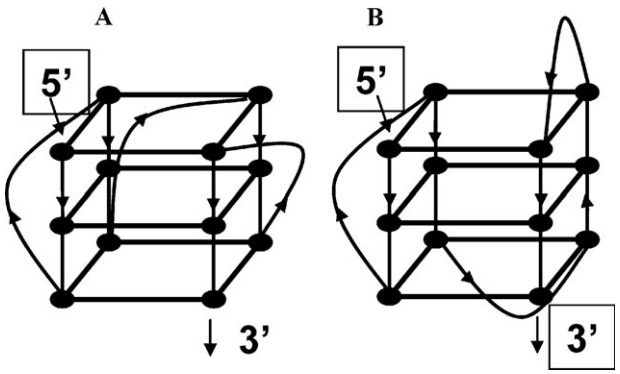

Scheme 2 Folding topologies of intramolecular human telomeric G-quadruplexes. (A) Parallel propeller with three external loops. (B) Parallel/antiparallel hybrid with one external and two lateral loops.

those in the absence of PEG, the Soret bands of both porphyrins are red-shifted by about 2 nm and the intensities are slightly increased in the presence of PEG (Fig. S1),† which are attributed to the change of the solvent polarity. It was reported that the Soret band of porphyrin will have a red shift and the intensities will increase as the solvent polarity decreases.[33]

In an attempt to determine the number of ligand-binding sites, continuous variation analysis (Job plot) was performed. Fig. 3 shows that both TMPyP4 and TPrPyP4 form 2 : 1 complexes with an antiparallel/parallel hybrid structure of $AG_3(T_2AG_3)_3$ G-quadruplex in the absence of PEG, whereas 1.63 : 1 and 1.38 : 1 complexes for TMPyP4 and TPrPyP4 with a parallel-stranded structure of $AG_3(T_2AG_3)_3$ G-quadruplex are formed in the presence of PEG, respectively.

Furthermore, the absorption titration data obtained were fit to the Scatchard model using eqn (1) (see Experimental section) (Fig. S2†). All Scatchard plots are nonlinear, which may be due to the unequal association constants of porphyrins for the different binding sites in G-quadruplexes. In order to confirm this hypothesis we use eqn (2) (see Experimental section) to construct the direct plots (Fig. S3).† In the absence and presence of PEG, the titration of TMPyP4 with $AG_3(T_2AG_3)_3$ gives the good fit curves, as expected, the interactions of TMPyP4 with parallel and antiparallel/parallel hybrid structures of $AG_3(T_2AG_3)_3$ present two types of binding, and one binding does not influence the binding on another site. Interestingly, a recent crystal structure reported by Neidle *et al.* also observed two independent binding sites for TMPyP4 in the complex with a human telomeric G-quadruplex DNA.[17]

According to the fitting results of eqn (2), the binding affinity of TMPyP4 for site 1 (K_1) is about two orders of magnitude smaller than that for site 2 (K_2) for both parallel and antiparallel/parallel hybrid structures of the $AG_3(T_2AG_3)_3$ G-quadruplex (Table 1), which is consistent with the previous reports wherein porphyrin binding was indicated to present one secondary site with lower affinity.[34,35] More recently, the binding constants of some derivatives of porphyrin to c-MYC and telomeric G-quadruplexes have been determined, indicating that there are one higher and one lower affinity sites.[36,37]

The current results are substantial different from our previous results about interactions of TMPyP4 with antiparallel $AG_3(T_2AG_3)_3$ in 100 mM Na^+-containing buffer,[13] in which the binding stoichiometry is 4, and the binding of TMPyP4 to antiparallel $AG_3(T_2AG_3)_3$ G-quadruplex

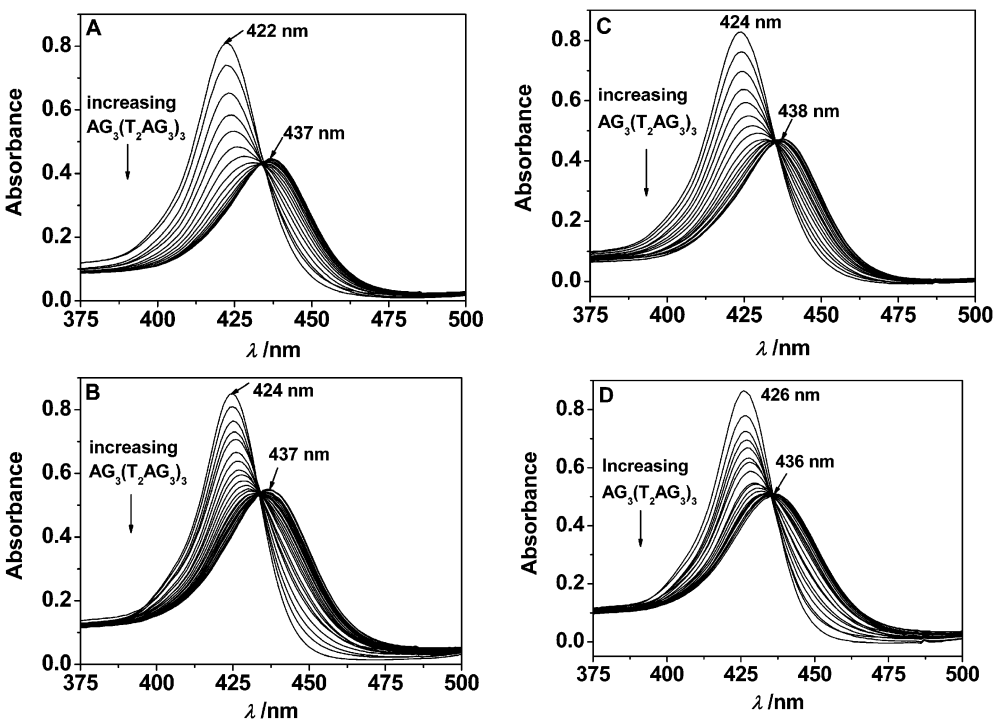

Fig. 2 Absorption titrations of 3.5 μM TMPyP4 (A, B) and TPrPyP4 (C, D) with $AG_3(T_2AG_3)_3$ in buffer containing 10 mM Tris-HCl (pH 7.5), 150 mM KCl, and 1mM EDTA in the absence (A, C) or presence of 40% PEG (B, D).

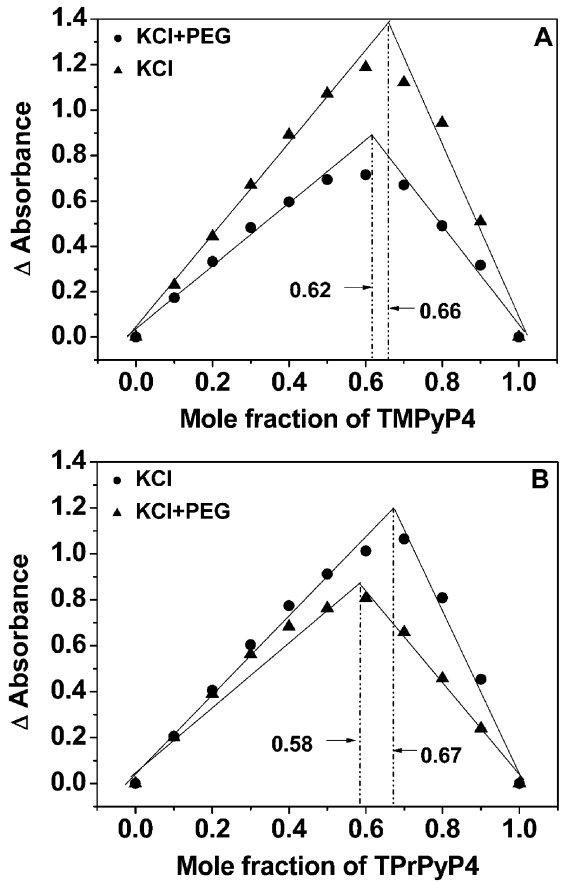

Fig. 3 Job plots of TMPyP4- (A) and TPrPyP4- (B) $AG_3(T_2AG_3)_3$ G-quadruplexes in 10 mM Tris-HCl (pH 7.5), 1 mM EDTA, and 150 mM K^+ buffer in the presence or absence of 40% PEG.

Table 1 The binding stoichiometries (n) and binding constants (K) of free porphyrins to G-quadruplexes in buffers containing 150 mM K^+ in the absence and presence of 40% PEG

Porphyrins	n_1	K_1/M^{-1}	n_2	K_2/M^{-1}
TMPyP4[a]	1.55[c]	1.07×10^{6}[c]	1.2[c]	4.42×10^{8}[c]
	1.48[d]	8.67×10^{5}[d]	0.54[d]	2.26×10^{8}[d]
TPrPyP4[b]	1.77[c]	1.24×10^{7}[c]	Undetected	Undetected
	1.64[d]	5.58×10^{6}[d]		

[a] n and K are obtained from eqn (2). [b] n and K are obtained from eqn (1). [c] In buffer without 40% PEG. [d] In buffer with 40% PEG.

is cooperative. This comparison reveals that both the binding mode and binding stoichiometry of TMPyP4 for the G-quadruplex depend on the structure of the G-quadruplex.

However, the bindings of TPrPyP4 to parallel and antiparallel/parallel hybrid structures of $AG_3(T_2AG_3)_3$ fail to give a satisfactory fit using eqn (2) (data not shown), which suggests a more complex binding behaviour between TPrPyP4 and $AG_3(T_2AG_3)_3$. To obtain the binding stoichiometries and association constants, data points at lower r values between 1.25 and 1.70 in the presence of PEG, between 0.95 and 1.50 in the absence of PEG were fit to the Scatchard plot (Fig. S2 C, D, insert),† and the fits give n values of 1.77 and 1.64, and the apparent association constants of 1.24×10^7 and 5.58×10^6 M^{-1} in the absence and presence of PEG, respectively (Table 1).

The binding stoichiometries shown in Table 1 are comparable with those obtained by the Job plot. The difference of the binding behaviour between TMPyP4 and TPrPyP4 with $AG_3(T_2AG_3)_3$ should arise from the difference of the size of the peripheral groups around the porphyrin core. It is obvious that one molecule bound to the G-quadruplex will affect another molecule binding to another site, that is, the cooperative effect is significant for TPrPyP4 with a large N-propyl substitute.

3.3 Binding modes of porphyrins to G-quadruplexes

On the basis of the absorption titration experiment, the values of hypochromicity % of both porphyrins are in the range of an intercalative binding (>35%), whereas the red-shift values are slightly smaller than those of the typical intercalation (>15 nm). In fact, the red shifts (>15 nm) and hypochromicities (>35%) given for intercalative binding modes were determined for long pieces of duplex DNA,[38] where the end stacking is not significant. So the red-shift value and hypochromicity associated with the binding stoichiometry and associate constant suggest that porphyrins interact with the G-quadruplex *via* terminal stacking and outside binding mode.

In order to provide further insight into the binding sites of both porphyrins for the G-quadruplex in the absence and presence of PEG, the steady-state and time-resolved fluorescence spectra were measured, which gives a more detailed information of the environment around a fluorophore.[39] Upon formation of complexes of porphyrins with G-quadruplexes at a G-quadruplex/porphyrin molar ratio of 3, their featureless broad bands are split in two peaks near 660 and 720 nm, and the ratio of intensity at 660 nm to that at 720 nm is also increased significantly (Fig. 4A). However, the emission bands of both free porphyrins are split in two peaks near 650 and 713 nm in a buffer containing PEG, which are red-shifted to 660 and 720 nm and the intensities are also decreased significantly upon addition of G-quadruplex (Fig. 4B), but the positions and intensity ratios of the emission peaks in the complexes are similar to those in the absence of PEG.

In the absence of PEG the featureless emission spectra of porphyrins are due to coupling the first excited state S_1 with a nearby charge transfer state CT from the porphyrin core to the pyridinium group.[40] Coupling is facilitated in high polarity solvents and by a high degree of rotational freedom of groups. The splitting of the Q(0,0) and Q(0,l) bands upon binding of porphyrins to DNA indicates that the electronic S_1–CT mixing within the bound excited molecule is less effective owing to a low polarity environment and confinement of porphyrin within the binding sites, thus hindering the free rotation of the *N*-methylpyridinium and *N*-propylpyridinium groups. Similarly, these also explain the band splitting of both porphyrins due to increase of solution viscidity and decrease of solution polarity in the presence of 40% PEG. A significant increase of the resolution of the Q(0,0) and Q(0,l) bands of porphyrins was also observed in methanol.[41]

It was reported that the outside bindings of TMPyP4 to both $[poly(dAdT)]_2$ and RNA result in a splitting and

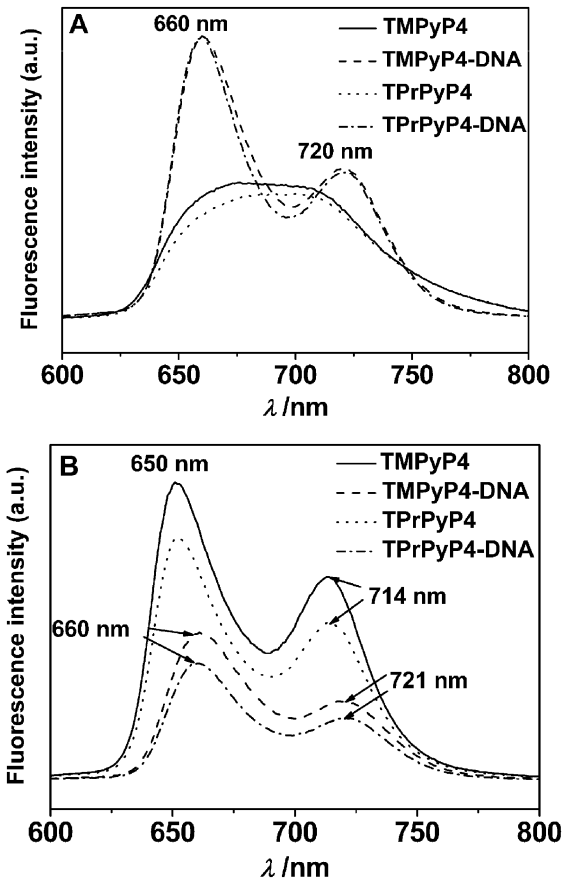

Fig. 4 Steady fluorescence spectra of free porphyrins at 4 μM and G-quadruplex–porphyrin complexes (G-quadruplex/porphyrin = 3 : 1) in a buffer solution containing 10 mM Tris-HCl (pH 7.5), 1 mM EDTA, and 150 mM K^+ in the absence (A) or presence of 40% PEG (B).

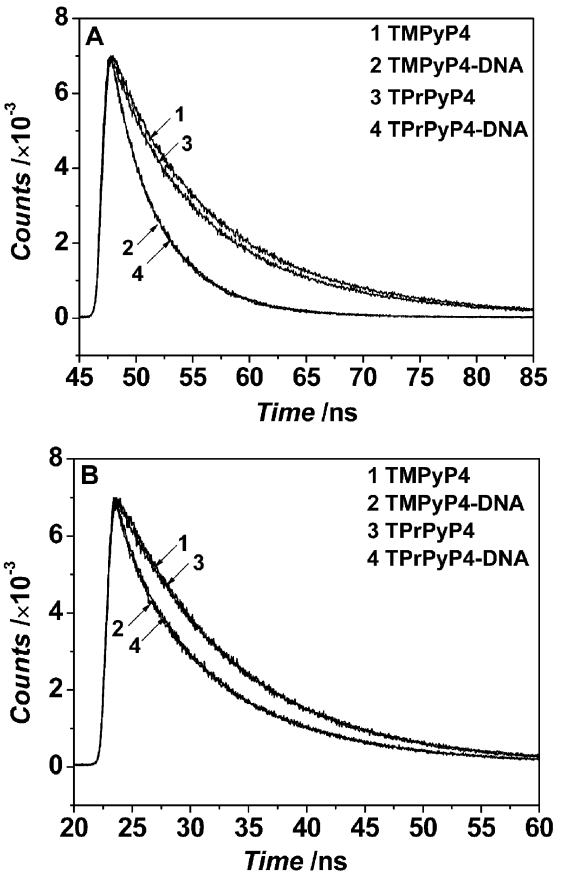

Fig. 5 Fluorescence decay curves of free porphyrins and G-quadruplex–porphyrin complexes (G-quadruplex/porphyrin = 3 : 1) in buffer solution containing 10 mM Tris-HCl (pH 7.5), 1 mM EDTA, and 150 mM K^+ in the absence (A) or presence of 40% PEG. They were obtained at 674 nm for free porphyrins and 660 nm for complexes in the absence of 40% PEG, 652 nm for free porphyrins and 660 nm for complexes in the presence of 40% PEG.

significant increase in intensity of the emission spectrum of TMPyP4.[42,43] The peak positions and ratios of Q(0,0) to Q(0,l) intensities are in good agreement with our present results. It is worthy of note that the fluorescence spectra of TMPyP4 in its complexes with $[poly(dG\text{-}dC)]_2$ and $[d(TACGTA)]_2$ are close to those obtained for $[poly(dAdT)]_2$,[44] but a ratio of Q(0,0) to Q(0,l) peak intensities and their red shift values were observed to increase in the order of $[poly(dG\text{-}dC)]_2 < [d(TACGTA)]_2 < [poly(dAdT)]_2$, which was explained by an increase of the proportion of externally bound porphyrins at the expense of intercalated ones. So these results further indicate that both porphyrins interact with G-quadruplexes by outside groove binding and terminal stacking.

Fig. 5 shows the fluorescence decays of porphyrins in the free form and complexes at 3 : 1 molar ratio of the G-quadruplex to the porphyrin, and their lifetime values are summarized in Table 2. For free TMPyP4 and TPrPyP4, the fluorescence decays are biexponential in the absence or presence of PEG (which consists in the reported results[45] where TMPyP4 in water and methanol gives rise to a biexponential fluorescence decay), which were attributed to the presence of two types of porphyrins: one is in solution and the other is the adsorbed molecules on the surface of the quartz cuvette. Here the shorter lifetimes of about 2 and 5–6 ns with the fractional amplitudes of about 10% originate from the adsorbed porphyrins, and the longer lifetimes of about 4–5 ns and 10–11 ns with the fractional amplitudes of about 90% are due to porphyrins in solution.

In the absence of PEG the fluorescence decays for G-quadruplex–porphyrin complexes are triexponential. Except for the shorter lifetime (about 3 ns, only 3–6%) which is still ascribed to the adsorbed porphyrin, there are another two longer lifetimes, which can be explained by two different localizations of the porphyrin molecules within the G-quadruplex DNA. Two lifetimes of porphyrins further support the existence of two types of binding modes obtained by an absorption titration fit. In addition, the number of adsorbed porphyrin molecules on the surface of the cell is remarkably decreased upon binding to G-quadruplexes and their lifetimes are also enhanced.

It was reported that the lifetimes of TMPyP4 molecules bound in duplex DNA are about 10 and 1.5 ns.[46–49] However assignments of both lifetimes to the intercalated or the externally bound porphyrins are inconsistent. Shen and coworkers[46] and Liu and coworkers[48] suggested that the shorter lifetime is the externally bound porphyrin, and the

Table 2 The fluorescence lifetimes of porphyrins in the free form and their complexes with G-quadruplexes in buffer solution containing 150 mM K^+ in the presence or absence of 40% PEG[a]

Compounds	Buffer	τ_1	τ_2	τ_3
TMPyP4	KCl	2.03 (16.82)	4.97 (83.18)	0
TMPyP4-DNA	KCl	2.76 (6.07)	7.45 (39.29)	12.43 (54.64)
TMPyP4	KCl + PEG	5.91 (9.83)	11.09 (90.17)	0
TMPyP4-DNA	KCl + PEG	0	3.56 (19.61)	10.74 (80.39)
TPrPyP4	KCl	2.01 (11.49)	4.63 (88.51)	0
TPrPyP4-DNA	KCl	2.83 (3.34)	6.60 (22.58)	11.84 (74.08)
TPrPyP4	KCl + PEG	5.26 (5.88)	10.53 (94.12)	0
TPrPyP4-DNA	KCl + PEG	0	2.92 (15.10)	10.60 (84.90)

[a] τ values denote the fluorescence lifetimes that were obtained at 674 nm for free porphyrins and 660 nm for complexes of $AG_3(T_2AG_3)_3$ with porphyrins in the absence of 40% PEG, 652 nm for free porphyrins and 660 nm for complexes of $AG_3(T_2AG_3)_3$ with porphyrins in the presence of 40% PEG. The data in bracket are the respective fractional amplitudes.

longer lifetime is the intercalated porphyrin, whereas the opposite viewpoint was suggested by Csík and coworkers[47] and Turpin and coworkers.[49] In addition, in the case of TMPyP4-[poly(dG-dC)]$_2$ complex, the decay kinetics are found to be doubly exponential and the lifetimes are 2.5 and 7.0 ns, which are markedly shorter than those of the complexes with [poly(dA-dT)$_2$ (12 ns).[49] It was found that the most probable types of interactions between porphyrin and [poly(dG-dC)]$_2$, and porphyrin and [poly(dA-dT)]$_2$ are the intercalation (containing end-stacking) and external (groove) binding, respectively. Taking these results into account, we identify the shorter lifetimes at 7.45 and 6.60 ns as belonging to the end-stacking species and the longer lifetimes at 12.43 and 11.84 ns as belonging to an externally bound porphyrin molecule in the groove.

However, in the presence of PEG the fluorescence decays for G-quadruplex–porphyrin complexes are biexponential. The fractional amplitudes of shorter lifetimes (3.56 and 2.92 ns) are increased from 9.83 and 5.88% to 19.6 and 15.1% for TMPyP4 and TPrPyP4 complexes with the G-quadruplex, respectively, and the corresponding lifetimes are decreased from 5.91 to 3.56 ns for the G-quadruplex–TMPyP4 complex and 5.26 to 2.92 ns for the G-quadruplex–TPrPyP4 complex, which are contrary to those in the absence of PEG. Thus we think that the shorter lifetime component does not belong to the adsorbed porphyrin molecules.

As described above, in the crowding condition the binding stoichiometries of both porphyrins to $AG_3(T_2AG_3)_3$ are lower than those in dilute buffer solution. According to the binding numbers of 1.4 and 1.6, we speculate, in the presence of 40% PEG, that one porphyrin molecule is stacked between two parallel-stranded $AG_3(T_2AG_3)_3$ G-quadruplexes to form sandwich complexes, which corresponds to the shorter lifetime component 3.56 (19.6%) and 2.92 (15.1%), another porphyrin molecule with the longer lifetime is bound to the groove of the G-quadruplex. This arrangement further explains that the lifetimes of porphyrin in the sandwich complex are shorter than those in end-stacking on the G-quartet of $AG_3(T_2AG_3)_3$ G-quadruplex.

The difference of the binding mode in the presence and absence of PEG comes from the different structure of the $AG_3(T_2AG_3)_3$ G-quadruplex. On the one hand, the crowding agent PEG may promote the formation of sandwich complexes; on the other hand, the parallel-stranded structure of the G-quadruplex is easy to interact with ligands *via* π–π stacking to form sandwich complexes.[17,50,51]

4. Conclusions

In summary, 40% PEG induces the structural transition of the $AG_3(T_2AG_3)_3$ G-quadruplex from an antiparallel/parallel hybrid structure to a parallel-stranded structure in buffer containing 150 mM K^+. Two independent and nonequivalent binding sites of TMPyP4 to parallel-stranded and antiparallel/parallel hybrid structures of $AG_3(T_2AG_3)_3$ G-quadruplex were confirmed, and the respective association constants are 1.07×10^6 and 4.42×10^8 M^{-1} for an antiparallel/parallel hybrid structure of $AG_3(T_2AG_3)_3$, 8.67×10^5 and 2.26×10^8 M^{-1} for a parallel-stranded $AG_3(T_2AG_3)_3$ G-quadruplex. However, interactions of TPrPyP4 with the $AG_3(T_2AG_3)_3$ G-quadruplex are cooperative in the absence and presence of 40% PEG, and the apparent association constants are 5.58×10^6 and 1.24×10^7 M^{-1} for a parallel-stranded and an antiparallel/parallel hybrid $AG_3(T_2AG_3)_3$ G-quadruplex, respectively. In the absence of PEG two TMPyP4 or TPrPyP4 molecules interact with the antiparallel/parallel hybrid $AG_3(T_2AG_3)_3$ G-quadruplex by external stacking and outside groove binding modes, whereas the sandwich structures are formed between two parallel-stranded $AG_3(T_2AG_3)_3$ G-quadruplexes and one porphyrin molecule in the presence of PEG, and another porphyrin molecule is bound to the groove of the parallel-stranded $AG_3(T_2AG_3)_3$ G-quadruplex.

Acknowledgements

This work was supported by the National Natural Science Foundation of China (20673110), the Natural Science Fund of the Shanxi Province (2009) and the Scientific Research Foundation for the Returned Overseas Chinese Scholars of the Shanxi Province (2007).

References

1 E. H. Blackburn, *Nature*, 1991, **350**, 569–573.
2 N. W. Kim, M. A. Piatyszek, K. R. Prowse, C. B. Harley, M. D. West, P. L. Ho, G. M. Coviello, W. E. Wright, S. L. Weinrich and J. W. Shay, *Science*, 1994, **266**, 2011–2015.
3 A. M. Zahler, J. R. Williamson, T. R. Cech and D. M. Prescott, *Nature*, 1991, **350**, 718–720.
4 H. Han and L. H. Hurley, *Trends Pharmacol. Sci.*, 2000, **21**, 136–142.
5 S. Neidle and G. Parkinson, *Nat. Rev. Drug Discovery*, 2002, **1**, 383–393.
6 N. Jing, W. Sha, Y. Li, W. Xiong and D. J. Tweardy, *Curr. Pharm. Des.*, 2005, **11**, 2841–2854.

7 E. M. Rezler, D. J. Bearss and L. H. Hurley, *Curr. Opin. Pharmacol.*, 2002, **2**, 415–423.
8 L. Oganesian and T. M. Bryan, *BioEssays*, 2007, **29**, 155–167.
9 W. D. Wilson and H. Sugiyama, *ACS Chem. Biol.*, 2007, **9**, 589–594.
10 E. Izbicka, R. T. Wheelhouse, E. Raymond, K. K. Davidson, R. A. Lawrence, D. Sun, B. E. Windle, L. H. Hurley and D. D. Von Hoff, *Cancer Res.*, 1999, **59**, 639–644.
11 N. V. Anantha, M. Azam and R. D. Sheardy, *Biochemistry*, 1998, **37**, 2709–2714.
12 I. Haq, J. O. Trent, B. Z. Chowdhry and T. C. Jenkins, *J. Am. Chem. Soc.*, 1999, **121**, 1768–1779.
13 C. Wei, G. Jia, J. Yuan, Z. Feng and C. Li, *Biochemistry*, 2006, **45**, 6681–6691.
14 R. T. Wheelhouse, D. Sun, H. Han, F. X. Han and L. H. Hurley, *J. Am. Chem. Soc.*, 1998, **120**, 3261–3262.
15 F. X. Han, R. T. Wheelhouse and L. H. Hurley, *J. Am. Chem. Soc.*, 1999, **121**, 3561–3570.
16 H. Han, D. R. Langley, A. Rangan and L. H. Hurley, *J. Am. Chem. Soc.*, 2001, **123**, 8902–8913.
17 G. N. Parkinson, R. Ghosh and S. Neidle, *Biochemistry*, 2007, **46**, 2390–2397.
18 K. Luby-Phelps, *Int. Rev. Cytol.*, 2000, **192**, 189–221.
19 S. B. Zimmerman and S. O. Trach, *J. Mol. Biol.*, 1991, **222**, 599–620.
20 A. P. Minton, *J. Biol. Chem.*, 2001, **276**, 10577–10580.
21 R. J. Ellis, *Trends Biochem. Sci.*, 2001, **26**, 597–604.
22 L. M. Charlton, C. O. Barnes, C. Li, J. Orans, G. B. Young and G. J. Pielak, *J. Am. Chem. Soc.*, 2008, **130**, 6826–6830.
23 Z. Kan, Y. Yao, P. Wang, X. Li, Y. Hao and Z. Tan, *Angew. Chem., Int. Ed.*, 2006, **45**, 1629–1632.
24 Y. Xue, Z. Kan, Q. Wang, Y. Yao, J. Liu, Y. Hao and Z. Tan, *J. Am. Chem. Soc.*, 2007, **129**, 11185–11191.
25 J. Zhou, C. Wei, G. Jia, X. Wang, Q. Tang, Z. Feng and C. Li, *Biophys. Chem.*, 2008, **136**, 124–127.
26 C. Wei, G. Han, G. Jia, J. Zhou and C. Li, *Biophys. Chem.*, 2008, **137**, 19–23.
27 T. A. Gray, K. T. Yue and L. G. Marzilli, *J. Inorg. Biochem.*, 1991, **41**, 205–219.
28 J. B. Chaires, *Methods Enzymol.*, 2001, **340**, 3–22.
29 L. R. Keating and V. A. Szalai, *Biochemistry*, 2004, **43**, 15891–15900.
30 K. C. Ingham, *Anal. Biochem.*, 1975, **68**, 660–663.
31 S. Paramasivan, I. Rujan and P. H. Bolton, *Methods*, 2007, **43**, 324–331.
32 A. Ambrus, C. Ding, J. Dai, T. Bialis, R. A. Jones and D. Yang, *Nucleic Acids Res.*, 2006, **34**, 2723–2735.
33 M. Makarska-Bialokoz, G. Pratviel and St. Radzki, *J. Mol. Struct.*, 2008, **875**, 468–477.
34 J. Seenisamy, S. Bashyam, V. Gokhale, H. Vankayalapati, D. Sun, A. Siddiqui-Jain, N. Streiner, K. Shin-Ya, E. White, W. D. Wilson and H. L. Hurley, *J. Am. Chem. Soc.*, 2005, **127**, 2944–2959.
35 T. Yamashita, T. Uno and Y. Ishikawa, *Bioorg. Med. Chem.*, 2005, **13**, 2423–2430.
36 K. Halder and S. Chowdhury, *Biochemistry*, 2007, **46**, 14762–14770.
37 I. M. Dixon, F. Lopez, A. M. Tejera, J.-P. Estève, M. A. Blasco, G. Pratviel and B. A. Meunier, *J. Am. Chem. Soc.*, 2007, **129**, 1502–1503.
38 R. F. Pasternack, E. J. Gibbs and J. J. Villafranca, *Biochemistry*, 1983, **22**, 2406–2414.
39 T. Lenz, E. Y. M. Bonnist, G. Pljevalji;, R. K. Neely, D. T. F. Dryden, A. J. Scheidig, A. C. Jones and E. Weinhold, *J. Am. Chem. Soc.*, 2007, **129**, 6240–6248.
40 K. Lang, J. Mosinge and D. M. Wagnerová, *Coord. Chem. Rev.*, 2004, **248**, 321–350.
41 K. Kano, T. T. Miyake, K. Yomoto, T. Sato, T. Ogawa and S. Hashimoto, *Chem. Lett.*, 1983, 1867–1870.
42 A. A. Ghazaryan, Y. B. Dalyan, S. G. Haroutiunian, A. Tikhomirova, N. Taulier, J. W. Wells and T. V. Chalikian, *J. Am. Chem. Soc.*, 2006, **128**, 1914–1921.
43 J. M. Kelly, M. J. Murphy, D. J. Mcconnell and C. A. Ohuigin, *Nucleic Acids Res.*, 1985, **13**, 167–184.
44 N. N. Kruk, S. I. Shishporenok, A. A. Korotky, V. A. Galievsky, V. S. Chirvony and P.-Y. Turpin, *J. Photochem. Photobiol., B*, 1998, **45**, 67–74.
45 F. J. Vergeldt, R. B. M. Koehorst, A. van Hoek and T. J. Schaafsma, *J. Phys. Chem.*, 1995, **99**, 4397–4405.
46 Y. Shen, P. Myslinski, T. Treszczanovicz, Y. Liu and J. A. Koningstein, *J. Phys. Chem.*, 1992, **96**, 7782–7787.
47 K. Zupán, L. Herényi, K. Tóth, Z. Majer and G. Csík, *Biochemistry*, 2004, **43**, 9151–9159.
48 Y. Liu, J. A. Koningstein and Y. Yevdokimov, *Can. J. Chem.*, 1991, **69**, 1791–1803.
49 V. S. Chirvony, V. A. Galievsky, N. N. Kruk, B. M. Dzhagarov and P.-Y. Turpin, *J. Photochem. Photobiol., B*, 1997, **40**, 154–162.
50 N. H. Campbell, G. N. Parkinson, A. P. Reszka and S. Neidle, *J. Am. Chem. Soc.*, 2008, **130**, 6722–6724.
51 G. N. Parkinson, F. Cuenca and S. Neidle, *J. Mol. Biol.*, 2008, **381**, 1145–1156.